NUMERICAL COMPUTATION OF THE TIME NON-LINEAR FRACTIONAL GENERALIZED EQUAL WIDTH MODEL ARISING IN SHALLOW WATER CHANNEL

by

***Nguyen Huu CAN*[a], *Omid NIKAN*[a], *Mohammad Navaz RASOULIZADEH*[b], *Hossein JAFARI*[c,d*], *and Yusif S. GASIMOV*[e,f,g]**

[a] Applied Analysis Research Group, Faculty of Mathematics and Statistics, Ton Duc Thang University, Ho Chi Minh City, Vietnam
[b] Department of Mathematics, Faculty of Basic Sciences, Velayat University, Iranshar, Iran
[c] Institute of Research and Development, Duy Tan University, Da Nang, Vietnam
[d] Department of Mathematical Sciences, University of South Africa, UNISA, Pretoria, South Africa
[e] Azerbaijan University, Baku, Azerbaijan
[f] Institute of Mathematics and Mechanics, ANAS, Baku, Azerbaijan
[g] Institute for Physical Problems, Baku State University, Baku, Azerbaijan

Original scientific paper
https://doi.org/10.2298/TSCI20S1049C

The generalized equal width model is an important non-linear dispersive wave model which is naturally used to describe physical situations in a water channel. In this work, we implement the idea of the interpolation by radial basis function to obtain numerical solution of the non-linear time fractional generalized equal width model defined by Caputo sense. In this technique, firstly, a time discretization is accomplished via the finite difference approach and the non-linear term is linearized by a linearization method. Afterwards, with the help of the radial basis function approximation method is used to discretize the spatial derivative terms.The stability of the method is theoretically discussed using the von Neumann (Fourier series) method. Numerical results and comparisons are presented which illustrate the validity and accuracy of our proposed concepts.

Key words: non-linear time fractional generalized equal width model, stability, radial basis function-finite difference, Caputo fractional derivative,

Introduction

The non-linear time fractional generalized equal width model (TFGEWM) is an important non-linear dispersive wave model which is naturally used to describe physical situations in a water channel. The current paper deals with the approximated solution for the non-linear TFGEWM order α ($0 < \alpha \le 1$):

$$\frac{\partial^\alpha u(x,t)}{\partial t^\alpha} + \varepsilon u^p(x,t)\frac{\partial u(x,t)}{\partial x} - \mu \frac{\partial^3 u(x,t)}{\partial x^2 \partial t} = f(x,t), \ \ x \in \Omega = (a,b), \ \ 0 < t \le T \tag{1}$$

with initial condition:

$$u(x,0) = f(x), \ \ x \in \bar{\Omega} = [a,b] \tag{2}$$

and the boundary conditions:

* Corresponding author, e-mail: jafarh@unisa.ac.za

$$u(a,t) = g_1(t),\ u(b,t) = g_2(t),\ t > 0 \tag{3}$$

where μ and ε are positive constants and $f(x, t)$ is a source term. The symbol $\partial^\alpha u(x, t)/\partial t^\alpha$ is the Caputo fractional derivative [1] which could be written:

$$\frac{\partial^\alpha u(x,t)}{\partial t^\alpha} = \begin{cases} \dfrac{1}{\Gamma(1-\alpha)} \displaystyle\int_0^t \frac{\partial u(x,\zeta)}{\partial \zeta} \frac{1}{(t-\zeta)^\alpha} \mathrm{d}\zeta, & 0 < \alpha < 1 \\[2ex] \dfrac{\partial u(x,t)}{\partial t}, & \alpha = 1 \end{cases}$$

When $\alpha \to 1$, eq. (1) converts to the GEWM, where p is a positive integer, ε and μ are positive parameters that need the boundary conditions $u \to 0$ as $x \to \pm\infty$. The GEWM was introduced as an alternative to generalized regularized long wave model and the generalized Korteweg-de Vries model [2, 3] to investigate soliton phenomena and as a model for small-amplitude long waves on the surface of water in a channel by Peregrine [4, 5] and Benjamin *et al*. [6]. The investigation of GEWM extends the opportunity of studying the construction of secondary solitary waves and/or radiation obtain intuition in the corresponding developments of particle physic [7]. This model attracted an increasing attention in physical situations such as long waves in near-shore zones, unilateral waves propagating in a water channel, and many others. For the special case $p = 1$, the GEWM model becomes the EWM [8] and for $p = 2$, the GEWM gets the modified EWM [9].

In recent years, fractional-order models have gained considerable popularity and importance in various fields of science and engineering [1]. Numerous scientific fields, such as mathematics and engineering make use of fractional calculus in applications such as anomalous diffusion and signal processing. Since phenomena can be described more accurately via fractional derivative. Due to this reasons, the analytical and numerical methods have increasingly been used to solve fractional models, see [10-20].

The main aim of this work is to construct a computational approach based on the radial basis function (RBF) to solve the non-linear TFGEWM.

Numerical formulation

To construct the numerical solution of eq. (1), we consider a uniform grid of spatial mesh points $\{x_j = jh | j = 1, 2, 3,..., N\}$ in the bounded domain [a, b], where x_1, x_N are the boundary points, and the spatial mesh points [0, T] are tagged as $t^n = n\delta t$, $n = 0, 1, 2, 3, ..., M$, where $h = (b - a)/\mathrm{N}$, $\delta t = T/M$, and $u^n = u^n(x_i) = u(x_i, t^n)$.

Time discretization strategy

Inspired by [20], the approximation of temporal fractional derivative term appearing in eq. (1) was discretized:

$$\frac{\partial^\alpha u(x,t^{n+1})}{\partial t^\alpha} = \begin{cases} a_\alpha (u^{n+1} - u^n) + a_\alpha \displaystyle\sum_{k=1}^{n} (u^{n+1-k} - u^{n-k}), & n \geq 1 \\[2ex] a_\alpha (u^1 - u^0), & n = 0 \end{cases} + \mathcal{O}(\delta t^{2-\alpha}) \tag{4}$$

where

$$a_\alpha = \frac{\delta t^{-\alpha}}{\Gamma(2-\alpha)}, \; b_k = (k+1)^{1-\alpha} - k^{1-\alpha} k = 0,1,\ldots,n$$

The time derivative of non-linear TGEWM is discretized by means of the common finite difference (FD) formula, which consists of space derivatives using the θ-weighted ($0 \le \theta \le 1$) scheme between two successive times n and $n+1$:

$$\frac{\partial^\alpha u\left(x, t^{n+1}\right)}{\partial t^\alpha} + \theta(\varepsilon u^p u_x)^{n+1} + (1-\theta)(\varepsilon u^p u_x)^n - \frac{\mu}{\delta t}\left(u_{xx}^{n+1} - u_{xx}^n\right) = f^{n+1} \tag{5}$$

where $u(x, t^{n+1}) = u^{n+1}, f(x, t^{n+1}) = f^{n+1}$, and $t^{n+1} = t^n + \delta t$.

Lemma 1. The non-linear term $(u^p u_x)^{n+1}$ can be linearized [21]:

$$(u^p u_x)^{n+1} \approx (u^p)^n u_x^{n+1} + p\left(u^{p-1}\right)u_x^n u^{n+1} - p(u^p)^n u_x^n + \mathcal{O}\left(\delta t^2\right), \quad p = 1,2,\ldots. \tag{6}$$

Substituting from eqs. (4) and (6) into eq. (5), we obtain:

$$\begin{aligned}&\left[a_\alpha \delta t + \theta \delta t \varepsilon p (u^n)^{p-1} u_x^n\right] u^{n+1} + \left[\theta \delta t \varepsilon (u^n)^p\right] u_x^{n+1} - \mu u_{xx}^{n+1} = a_\alpha \delta t u^n + \\ &+ \delta t \varepsilon\left[(p+1)\theta - 1\right](u^n)^p u_x^n - \mu u_{xx}^n - a_\alpha \delta t \sigma^n + \delta t f^{n+1}, \quad n = 0,1,\ldots\end{aligned} \tag{7}$$

where

$$\sigma^0 = 0 \text{ and } \sigma^n = \sum_{k=1}^{n} b_k \left(u^{n+1-k} - u^{n-k}\right), \quad n \ge 1$$

Spatial discretization, the RBF collocation method in global mode (GRBF)

The RBF interpolation method uses linear combinations of translates of one function ϕ of a single real variable [21, 22]. The numerical approximation $u(x_i, t^n)$ at a point of interest x_i is expanded:

$$u(x_i, t^n) = u_i^n \simeq \sum_{j=1}^{N} \lambda_j^n \phi(r_{ij}) \tag{8}$$

where $\{\lambda_j^n\}$ are unknown coefficients of the n^{th} time layer $\phi(r_{ij})$ RBF, $r_{ij} = |x_i - x_j|$. The inverse multiquadric (IMQ) $1/(c^2 + r^2)^{1/2}$, inverse quadratic (IQ) $(c^2 + r^2)^{-1}$, and multiquadric (MQ) $(c^2 + r^2)^{1/2}$ is globally supported RBF where constant c are commonly known as the RBF shape parameter. The unknown coefficient vector λ_j^n, $j = 1,..., N$ will be obtained by the collocation method. The system (8) can be put in a matrix form as below:

$$\mathbf{u}^n = \mathbf{A}\lambda^n \tag{9}$$

One can split the matrix $\mathbf{A}$ into two matrices, namely $\mathbf{A}_b$ (matrix-associated boundary), and $\mathbf{A}_d$ (matrix-associated internal) which correspond to two boundary points and $N-2$ interior points:

$$\mathbf{A} + \mathbf{A}_d + \mathbf{A}_b$$

where

$$\mathbf{A}_d = \left[\phi\left(r_{ij}\right) : 2 \le i \le N-1, \; 1 \le j \le N \text{ and } 0 \text{ elsewhere}\right]$$

$$\mathbf{A}_b = \left[\phi\left(r_{ij}\right) : i = 1, N, \; 1 \le j \le N \text{ and } 0 \text{ elsewhere}\right]$$

By inserting eq. (8) into eq. (16), one gets the following equations in the interior points of the domain set $[a, b]$:

$$\left\{a_\alpha \delta t + \theta\delta t\varepsilon p\left[\sum_{j=1}^{N}\lambda_j^n\phi_j(x_i)\right]^{p-1}\sum_{j=1}^{N}\lambda_j^n\phi_j'(x_i)\right\}\sum_{j=1}^{N}\lambda_j^{n+1}\phi_j(x_i)+\left\{\theta\delta t\varepsilon\left[\sum_{j=1}^{N}\lambda_j^n\phi_j(x)\right]^p\right\}\cdot$$

$$\cdot\sum_{j=1}^{N}\lambda_j^{n+1}\phi_j'(x_i)-\mu\sum_{j=1}^{N}\lambda_j^{n+1}\phi_j''(x_i)=a_\alpha\delta t\sum_{j=1}^{N}\lambda_j^n\phi_j(x_i)+\delta t\varepsilon\left[(p+1)\theta-1\right]\left[\sum_{j=1}^{N}\lambda_j^n\phi_j(x)\right]^p\cdot$$

$$\cdot\sum_{j=1}^{N}\lambda_j^n\phi_j'(x_i)-\mu\sum_{j=1}^{N}\lambda_j^n\phi_j''(x_i)-a_\alpha\delta t\sum_{k=1}^{n}b_k(u^{n+1-k}-u^{n-k})+\delta tf^{n+1} \tag{10}$$

where

$$\phi'\left(r_{ij}\right)=\frac{\mathrm{d}}{\mathrm{d}x}\phi\left(\left|x-x_j\right|\right)|_{x=x_i},\ \ \phi''\left(r_{ij}\right)=\frac{\mathrm{d}^2}{\mathrm{d}x^2}\phi\left(\left|x-x_j\right|\right)|_{x=x_i},\quad i=2,3,\ldots,N-1$$

For the boundary points, we obtain the following relations:

$$\sum_{j=1}^{N}\lambda_j^{n+1}\phi_j(x_i)=g_1(t^{n+1}),\ \sum_{j=1}^{N}\lambda_j^{n+1}\phi_j(x_N)=g_2(t^{n+1}) \tag{11}$$

Rewriting eqs. (10) and (11) in a matrix form, it is to illustrate:

$$\left[a_\alpha\delta t\mathbf{A}_d+\mathbf{A}_b-\mu\mathbf{C}+\theta\delta t\varepsilon\left(\mathbf{D}+\mathbf{E}\right)\right]\lambda^{n+1}=\left(a_\alpha\delta t\mathbf{A}_d-\mu\mathbf{C}+\delta t\left\{\varepsilon\left[\left(p+1\right)\theta-1\right]\mathbf{E}\right\}\right)\lambda^n+\mathbf{G}^{n+1} \tag{12}$$

where

$$\mathbf{u}_x^n=\mathbf{B}\lambda^n,\ D=p(\mathbf{u}^n)^{p-1}\times\mathbf{u}_x^n\times\mathbf{A}_d,\ E=(\mathbf{u}^n)^p\times\mathbf{B}$$

$$\mathbf{B}=[\phi_j'\left(x_i\right):i=2,\ldots,N-1,\ \ j=1,\ldots,N\ \text{ and }\ 0\text{ elsewhere}]_{N\times N}$$

$$\mathbf{C}=[\phi_j''\left(x_i\right):i=2,\ldots,N-1,\ \ j=1,\ldots,N\ \text{ and }\ 0\text{ elsewhere}]_{N\times N}$$

$$\mathbf{G}^{n+1}=\mathbf{G}_1^{n+1}+\mathbf{G}_2^{n+1}+\mathbf{F}^{n+1}$$

$$\mathbf{G}_1^{n+1}=\left[g_1\left(t^{n+1}\right)0,...,0,g_2\left(t^{n+1}\right)\right]^T,\quad \mathbf{G}_2^{n+1}=\left\{-a_\alpha\delta t\sum_{k=1}^{n}b_k\left(\mathbf{u}^{n+1-k}-\mathbf{u}^{n-k}\right)\right\}^T$$

$$\mathbf{F}^{n+1}=\left[0,\delta tf_2^{n+1},\ldots,\delta tf_{N-1}^{n+1},0\right]$$

The accent × defines that the i^{th} component of the vector $\mathbf{u}^n$ is multiplied to every element of the i^{th} row of matrix. The relation (12) exhibits a system of N linear equations in N unknown coefficients λ_j. The numerical solution my be achieved from eq. (8) at any node in the interval $[a, b]$ posterior to obtaining the values of the unknown vector $\lambda_j, j = 1, 2,..., N$ at each time step.

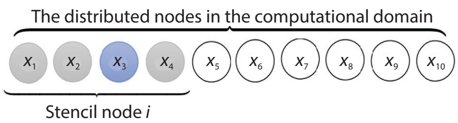

Figure 1. The schematic diagram for stencil in the 1-D computational domain

Spatial discretization, the local RBF in finite difference mode

This local RBF technique can be viewed as a generalized form of the traditional FD technique, hence, it is also known as the RBF-FD technique [21, 23]. For the convenience of marking, we assuming that $S^I = \{x_k^{(i)},...,x_{N_I}^{(i)}\} \subseteq \zeta$ be the local support domain (stencil), and every point $x_k^{(i)}$ corresponds to a point x_i in the collection points set $\zeta = \{x_1,...,x_N\}$ that be an uniform partition of $[a, b]$ where $x_1 = a$ and $x_N = b$.

The derivatives of function $u^k(x)$ can be represented approximately applying only function values in the stencil of x_i:

$$\frac{\partial u^k(x)}{\partial x}|_{x=x_i} = \sum_{j=1}^{N_I} \omega_{i,j}^{x,1} u^k(x_j^i), \quad \frac{\partial^2 u^k(x)}{\partial x^2}|_{x=x_i} = \sum_{j=1}^{N_I} \omega_{i,j}^{x,2} u^k(x_j^i) \tag{13}$$

where $w_{i,j}^{x,1}$ and $w_{i,j}^{x,2}$ denote the RBF-FD coefficients corresponding to the first and second order derivatives with respect to x, and N_I is the number of nodes in the stencil of i^{th} node. The RBF-FD stencil of size N_I requires the $N_I - 1$ nearest neighbors, see fig. 1. By replacing relations (13) in eq. (16) and collocating it in for time steps $k = n$, $n + 1$ yields in the following time semi-discretization equation:

$$\left\{a_\alpha \delta t + \theta \delta t \varepsilon p \left[u^n(x_i)\right]^{p-1} \sum_{j=1}^{N_I} \omega_{i,j}^{x,1} u^n(x_i)\right\} u^{n+1}(x_i) + \left\{\theta \delta t \varepsilon \left[u^n(x_i)\right]^p\right\} \sum_{j=1}^{N_I} \omega_{i,j}^{x,1} u^{n+1}(x_j) -$$

$$-\mu \sum_{j=1}^{N_I} \omega_{i,j}^{x,2} u^{n+1}(x_j) = a_\alpha \delta t u^n(x_i) + \delta t \varepsilon \left[(p+1)\theta - 1\right]\left[u^n(x_i)^p\right] \sum_{j=1}^{N_I} \omega_{i,j}^{x,1} u^n(x_j) -$$

$$-\mu \sum_{j=1}^{N_I} \omega_{i,j}^{x,2} u^n(x_j) = a_\alpha \delta t \sum_{k=1}^{n} b_k \left[u^{n+1-k}(x_i) - u^{n-k}(x_i)\right] + \delta t f^{n+1}(x_i) \tag{14}$$

After imposing the boundary conditions, we can write the aforementioned relations in the matrix notation:

$$\mathbf{A} u^{n+1} = \mathbf{B} u^n + \mathbf{F} \tag{15}$$

where the elements of **A**, **B**, and **F** are

$$a_{ii} = \left[a_\alpha \delta t + \theta \delta t \varepsilon p (u_i^n)^{p-1} \sum_{j=1}^{N_I} \omega_{i,j}^{x,1} u^n(x_j)\right] + \left[\theta \delta t \varepsilon (u_i^n)^p\right] \omega_{ii}^{x,1} - \mu \omega_{ii}^{x,2}$$

$$a_{ij} = \left[\theta \delta t \varepsilon (u_i^n)^p\right] w_{ij}^{x,1} - \mu w_{ij}^{x,2}$$

$$b_{ii} = a_\alpha \delta t u_i^n + \delta t \varepsilon \left[\left(p+1\right)\theta - 1\right](u_i^n)^p w_{ii}^{x,1} - \mu w_{ii}^{x,2}$$

$$b_{ij} = \delta t \varepsilon \left[\left(p+1\right)\theta - 1\right](u_i^n)^p w_{ij}^{x,1} - \mu w_{ij}^{x,2}$$

$$F_i^{n+1} = -a_\alpha \delta t \sum_{k=1}^{n} b_\alpha(k) \left[u^{n-k+1}\left(x_i\right) - u^{n-k}\left(x_i\right)\right] + \delta t f_i^{n+1}$$

If boundary node x_k is in the support domain of node x_i then F is updated:

$$F_i^{n+1} = -a_\alpha \delta t \sum_{k=1}^{n} b_\alpha(k)(u_i^{n-k+1} - u_i^{n-k}) + \delta t f_i^{n+1} - \left[\theta \delta t \varepsilon (u_i^n)^p\right] \omega_{ik}^{x,1} + \mu \omega_{ik}^{x,2}$$

The stability of the numerical scheme

In this section, we will describe the stability of the proposed numerical solution. In the non-linear convective term, we must first freeze one variable locally, then use the standard Fourier analysis to obtain the condition for stability to be imposed on the time step δt. By applying the proposed method for the locally constant equation in the case $f \equiv 0$:

$$\left(a_\alpha \delta t+\theta\delta t\varepsilon p\mathcal{A}^{p-1}\mathcal{B}\right)u^{n+1}+\theta\delta t\varepsilon\mathcal{B}^p u_x^{n+1}-\mu u_{xx}^{n+1}=a_\alpha \delta t u^n+$$

$$+\delta t\left\{\varepsilon\left[\left(p+1\right)\theta-1\right]\mathcal{B}^p\right\}u_x^n-\mu u_{xx}^n-a_\alpha\delta t\sum_{k=1}^{n}b_k\left(u^{n+1-k}-u^{n-k}\right) \tag{16}$$

where $\mathcal{A}=u^n$, $\mathcal{B}=u_x^n$.

In view of the Von Neumann's method for each j by taking $u_j^n=\zeta^n e^{\ell\varphi xj}$ and substituting in eq. (16), and after simplifying we obtain:

$$\zeta=\frac{\vartheta_1+\ell\kappa_1}{\vartheta_2+\ell\kappa_2} \tag{17}$$

where

$$\vartheta_1=\left(a_\alpha\delta t+\theta\delta t\varepsilon p\mathcal{A}^{p-1}\mathcal{B}\right)+\mu\varphi^2,\quad \kappa_1=\theta\delta t\varepsilon\mathcal{B}^p\varphi$$

$$\vartheta_2=a_\alpha\delta t+\mu\varphi^2-a_\alpha\delta t\sum_{k=1}^{n}b_k\left(\zeta^{1-k}-\zeta^{-k}\right),\quad \kappa_2=\delta t\left\{\varepsilon\left[\left(p+1\right)\theta-1\right]\right\}\mathcal{B}^p\varphi$$

so that ℓ denotes the imaginary unit and φ is real:

$$|\zeta|^2=\frac{\vartheta_1^2+\kappa_1^2}{\vartheta_2^2+\kappa_2^2}=\frac{P}{Q}=\frac{P}{P+\left(Q-P\right)} \tag{18}$$

In the aforesaid relation by choosing $\theta = 1/2$ and after simplifying, the inequality $(Q-P)\geq 0$ holds. Consequently, it concludes that $|\zeta|\leq 1$ [21]. Therefore, the necessary condition for the stability is provided and we can state that our method is convergence.

Results and discussion

This section presents one prototype example to show the efficiency and the validation the techniques discussed in the previous section. To measure the accuracy of the schemes, we compute the following error norms:

$$L_\infty=\max_{1\leq j\leq N-1}|u_j-U_j|,\ RMS=\left[\frac{1}{N}\sum_{j=1}^{N}(u_j-U_j)^2\right]^{1/2}$$

where $u_j = u(x_j, T)$, $U_j = (x_j, T)$ are the exact and approximate solutions, respectively. The conservation property belonging to the TFGEWE will be assessed through to show that the algorithm is significant the estimation of quantities pertaining to mass, momentum, and energy conservation:

$$I_1=h\sum_{i=1}^{N}U_i,\ I_2=h\sum_{i=1}^{N}\left[(U_i)^2+\mu(u_{xi})^2\right],\quad I_3=h\sum_{i=1}^{N}(U_i)^{p+2}$$

Let us consider the non-linear TFGEWM:

$$\frac{\partial^\alpha u\left(x,t\right)}{\partial t^\alpha}+3u^2\left(x,t\right)\frac{\partial u\left(x,t\right)}{\partial x}-\mu\frac{\partial^3 u\left(x,t\right)}{\partial x^2\partial t}=0,\quad 0\leq t\leq T,\quad 0<\alpha<1$$

with an initial conditions:

$$u\left(x,0\right)=A_0\operatorname{sech}\left(\nu x\right),\quad \mu=\frac{1}{\nu^2}$$

where μ is a positive value and the subscripts x and t denote differentiation [24]. For the special case $\alpha = 1$, the aforementioned fractional equation becomes the classical modified EWM with the exact solution $u(x, t) = A_0\text{sech}[\nu(x - \omega t)]$ where $\omega = A_0^2/2$. Table 1 reports the RMS error and L_∞ error of the approximated solutions. It can be mentioned that the numerical results obtained by the RBF-FD method are in close agreement with the exact solution. On the other hand, the interpolation matrix of the RBF-FD method is a sparse and well-conditioned matrix when increase the number of nodes can be increased. The conservation quantities I_1, I_2, and I_3 obtained are illustrated in tab. 2. From the numerical results given in tab. 2, it can be noted that the conservation values remains constant during the simulation. Figures 2 and 3 plot the numerical solutions and errors L_∞ obtained with with values of $A_0 = 0.05$ and 0.1, $\nu = 1$, $\alpha = 0.9$ and $x \in [-1.2, 1.2]$ by using our proposed schemes. We can see that the error observed in the GRBF method increases more than when using the RBF-FD method. In addition, the characteristics of figs. 2 and 3 are consistent with [24, fig. 2]. In addition, tab. 3 demonstrates the L_∞ error for MQ-RBF and IQ-RBF. It is worthy of note that we employed only the first eight terms of the series (as an exact solution) achieved from DTM method in [24] for the obtained numerical results.

Table 1. The numerical errors in the solution with $\delta t = 0.01$ and $\theta = 1/2$

Methods	T	c	N	N_I	Cond(M)	L_∞	RMS
RBF-FD	1	0.65	200	55	$5.8113 \cdot 10^5$	$9.7715 \cdot 10^{-6}$	$7.4482 \cdot 10^{-6}$
GRBF	1	0.65	200	–	$1.6745 \cdot 10^{18}$	$1.4391 \cdot 10^{-4}$	$8.6930 \cdot 10^{-5}$
RBF-FD	2	0.65	200	55	$5.8113 \cdot 10^5$	$4.3439 \cdot 10^{-5}$	$3.3507 \cdot 10^{-5}$
GRBF	2	0.65	200	–	$1.6745 \cdot 10^{18}$	$4.3574 \cdot 10^{-4}$	$3.2931 \cdot 10^{-4}$
RBF-FD	3	0.50	200	55	$5.8113 \cdot 10^5$	$8.7382 \cdot 10^{-5}$	$6.6727 \cdot 10^{-5}$
GRBF	3	0.50	200	–	$1.6745 \cdot 10^{18}$	$8.6637 \cdot 10^{-4}$	$6.6055 \cdot 10^{-4}$
RBF-FD	4	0.90	200	55	$5.8113 \cdot 10^5$	$1.2738 \cdot 10^{-4}$	$9.7154 \cdot 10^{-5}$
GRBF	4	0.90	200	–	$1.6745 \cdot 10^{18}$	$1.2673 \cdot 10^{-3}$	$9.6583 \cdot 10^{-4}$

Table 2. Invariant quantities by choosing $A_0 = 0.1$, $h = 0.01$, $\nu = 1$, $\alpha = 0.5$, and $x \in [-1.2, 1.2]$ for c = 0.95 for single solitary wave

δt	[24]			Present method		
	I_1	I_2	I_3	I_1	I_2	I_3
0.00	0.19840108	0.01989219	0.00012931	0.19851138	0.02063038	0.00012873
0.01	0.19840107	0.01989220	0.00012931	0.19851186	0.02063057	0.00012873
0.02	0.19840105	0.01989220	0.00012931	0.19851180	0.02063048	0.00012873
0.03	0.19840104	0.01989221	0.00012931	0.19851180	0.02063056	0.00012873
0.04	0.19840102	0.01989221	0.00012931	0.19851245	0.02063054	0.00012872
0.05	0.19840100	0.01989221	0.00012931	0.19851168	0.02063048	0.00012872
0.06	0.19840099	0.01989222	0.00012931	0.19851281	0.02063048	0.00012872
0.07	0.198401097	0.01989222	0.00012931	0.19851038	0.02063047	0.00012872
0.08	0.198401096	0.01989223	0.00012931	0.19851861	0.02063047	0.00012872

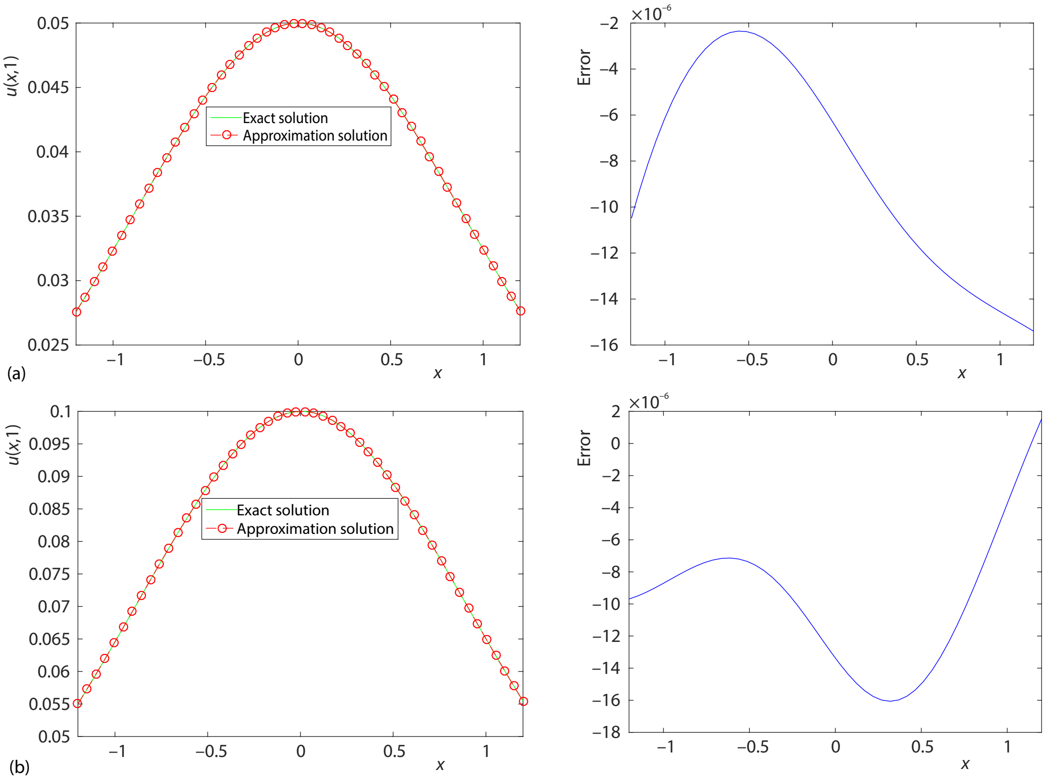

Figure 2. The approximate solutions and evaluated errors for (a) $A_0 = 0.05$, (b) $A_0 = 0.1$ with $\alpha = 0.9$, $h = 0.1$, $\nu = 1$, $\delta t = 0.05$, $c = 0.96$ and $x \in [-1.2, 1.2]$ by using RBF-FD method at $T = 1$

Table 3. The numerical errors using MQ-RBF and IQ-RBF with $A_0 = 0.05$, $\nu = 1$, $\alpha = 0.9$, and $x \in [-1.2, 1.2]$ at $T = 10$, and $h = 0.01$

δt	*MQ*		*IQ-RBF*	
	c	L_∞	c	L_∞
8/10	1.00	$2.2493 \cdot 10^{-3}$	0.90	$5.5563 \cdot 10^{-3}$
4/10	1.00	$1.1106 \cdot 10^{-3}$	0.90	$2.7172 \cdot 10^{-3}$
2/10	0.90	$5.2511 \cdot 10^{-4}$	0.85	$1.3514 \cdot 10^{-3}$
1/10	0.90	$2.5741 \cdot 10^{-4}$	0.90	$6.5241 \cdot 10^{-4}$
5/100	0.85	$1.2068 \cdot 10^{-4}$	0.90	$3.1712 \cdot 10^{-4}$
5/200	1.00	$5.5988 \cdot 10^{-5}$	1.00	$1.5177 \cdot 10^{-4}$

Conclusion

This paper adopted the effect of the fractional order derivative on the structure and propagation of the resulting solitary waves obtained from TFGEWM. The numerical results obtained in section *Results and discussion* and the comparisons between them and several other techniques indicate the considerable accuracy of proposed approach. The results obtained from the RBF-FD technique are somewhat similar to those obtained from the GRBF technique. The

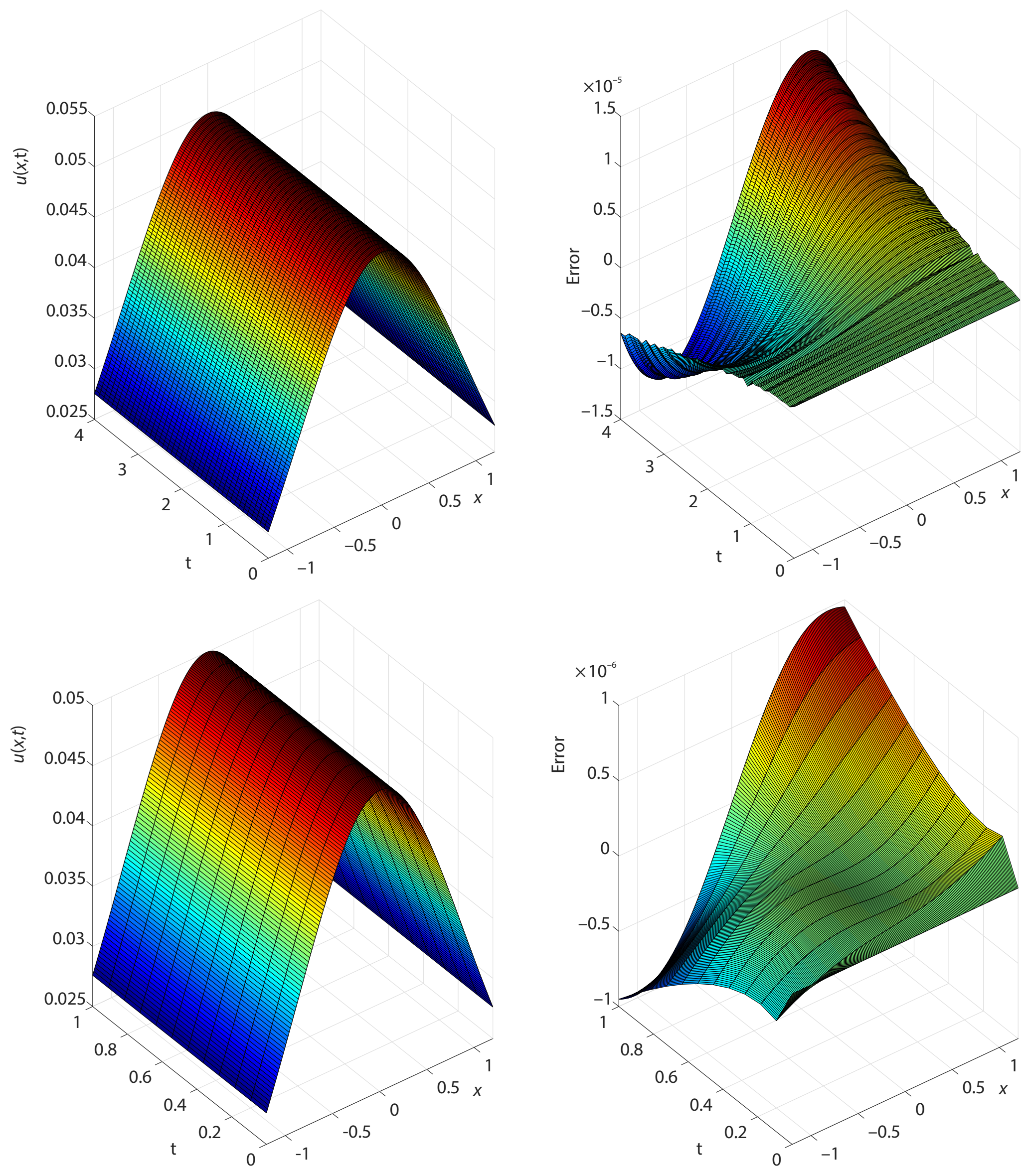

Figure 3. Graphs of approximation solution and resulted error for $A_0 = 0.05$, $\nu = 1$, $\alpha = 0.9$, and $x \in [-1.2, 1.2]$ by using GRBF method with $h = 0.05$, $\delta t = 0.005$, and $c = 0.75$

system matrix corresponding to the GRBF technique is ill-conditioned and dense. Contrarily, a well-conditioned and sparse matrix is observed in the RBF technique. Therefore, the quantity of nodes in the RBF-FD technique may be increased to a certain level. Both of these techniques can be applied to high dimensional problems. It has been shown that the linearized scheme of the proposed approach is unconditionally stable using the linearized stability analysis.

References

[1] Oldham, K. B., Spanier, J., *The Fractional Calculus*, Mathematics in Science and Engineering, Elsavier, Amsterdam, The Netherlands, Vol. 111, 1974
[2] Kaya, D., A Numerical Simulation of Solitary-Wave Solutions of the Generalized Regularized Long-Wave Equation, *Applied Mathematics and Computation*, *149* (2004), 3, pp. 833-841
[3] Kaya, D., El-Sayed, S. M., An Application of the Decomposition Method for the Generalized KdV and RLW Equations, *Chaos, Solitons and Fractals*, *17* (2003), 5, pp. 869-877
[4] Peregrine, D., Calculations of the Development of an Undular Bore, *Journal of Fluid Mechanics*, *25* (1966), 2, pp. 321-330
[5] Peregrine, D. H., Long Waves on a Beach, *Journal of Fluid Mechanics*, *27* (1967), 4, pp. 815-827
[6] Benjamin,T. B., *et al*., Model Equations for Long Waves in Non-Linear Dispersive Systems, *Philosophical Transactions of the Royal Society of London A*, *272* (1972), 1220, pp. 47-78
[7] Courtenay Lewis, J., Tjon, J., Resonant Production of Solitons in the RLW Equation, *Physics Letters A*, *73* (1979), 4, pp. 275-279
[8] Zaki, S., A Least-Squares Finite Element Scheme for the EW Equation, *Computer Methods in Applied Mechanics and Engineering*, *189* (2000), 2, pp. 587-594
[9] Gardner, L., Gardner, G., Solitary Waves of the Equal Width Wave Equation, *Journal of Computational Physics*, *101* (1992), 1, pp. 218-223
[10] Inc, M., *et al*., Modified Variational Iteration Method for Straight Fins with Temperature Dependent Thermal Conductivity, *Thermal Science*, *22* (2018), Suppl. 1, pp. S229-S236
[11] Akgul, A., *et al*., New Method for Investigating the Density-Dependent Diffusion Nagumo Equation, *Thermal Science*, *22* (2018), Suppl. 1, pp. S143-S152
[12] Moallem, G. R., *et al*., A Numerical Scheme to Solve Variable Order Diffusion-Wave Equations, *Thermal Science*, *23* (2019), Suppl. 6, pp. S2063-S2071
[13] Ganji, R., Jafari, H., Numerical Solution of Variable Order Integro-Differential Equations, *Advanced Mathematical Models and Applications*, *4* (2019), 1, pp. 64-69
[14] Aziz, R., Kumawat, Y., Marichev-Saigo-Maeda Fractional Calculus Operators with Extended Mittag-Leffler Function and Generalized Galue Type Struve Function, *Advanced Mathematical Models and Applications*, *4* (2019), 3, pp. 210-223
[15] Jafari, H., Tajadodi, H., New Method for Solving a Class of Fractional Partial Differential Equations with Applications, *Thermal Science*, *22* (2018), Suppl. 1, pp. S277-S286
[16] Khan, H., *et al*., Existence and Data Dependence Theorems for Solutions of an ABC-Fractional Order Impulsive System, *Chaos, Solitons and Fractals*, *131* (2020), 109477
[17] Khan, A., *et al.*, Analytical Solutions of Time-Fractional Wave Equation by Double Laplace Transform Method, *The European Physical Journal Plus*, *134* (2019), 4, 163
[18] Khan, H., *et al*., A Singular ABC-Fractional Differential Equation with p-Laplacian Operator, *Chaos, Solitons and Fractals*, *129* (2019), Dec., pp. 56-61
[19] Khan, H., *et al*., A Fractional Order HIV-TB Coinfection Model with Non-Singular Mittag-Leffler Law, *Mathematical Methods in the Applied Sciences*, *43* (2020), 6, pp. 3786-3806
[20] Golbabai, A., *et al.*, Numerical Investigation of the Time Fractional Mobile-Immobile Advection-Dispersion Model Arising from Solute Transport in Porous Media, *International Journal of Applied and Computational Mathematics*, *5* (2019), 3, 50
[21] Rashidinia, J., Rasoulizadeh, M. N., Numerical Methods Based on Radial Basis Function-Generated Finite Difference (RBF-FD) for Solution of GKdVB Equation, *Wave Motion*, *90* (2019), Aug., pp. 152-167
[22] Fasshauer, G. E., *Meshfree Approximation Methods with MATLAB*: (With CD-ROM), World Scientific Publishing Company, Singapore, Vol. 6, 2007
[23] Tolstykh, A., Shirobokov, D., On Using Radial Basis Functions in A Finite Difference Mode with Applications to Elasticity Problems, *Computational Mechanics*, *33* (2003), 1, pp. 68-79
[24] Merdan, M., *et al*., Numerical Solution of Time-Fraction Modified Equal Width Wave Equation, *Engineering Computations*, *29* (2012), 7, pp. 766-777

Paper submitted: April 14, 2020
Paper revised: May 20, 2020
Paper accepted: May 26, 2020